Proceedings of the IMAC-XXVIII
February 1–4, 2010, Jacksonville, Florida USA

Estimating Effective Prestress Force on Grouted Tendon by Impact Responses

[*]Byeong Hwa Kim, [**]Soo Jin Kim, [**]Keum Soo Yeo, [***]Jung-Bum Jang and [***]Hong-Pyo Lee

[*]Assistant Professor, Department of Civil Engineering, Kyungnam University, 449 Wolyoung, Masan, Kyungnam, 631-701, Republic of Korea
[**]Master Student, Department of Civil Engineering, Kyungnam University, 449 Wolyoung, Masan, Kyungnam, 631-701, Republic of Korea
[***]Researcher, Structure Safety Group, Environment & Structure Laboratory, Korea Electric Power Research Institute, 103-16 Munji-Dong, Yuseong-Gu, Daejeon, 305-380, Republic of Korea.

ABSTRACT: A way of evaluating effective tensile force on a grouted seven-wire strand embedded in the post-tensioned beams has been examined experimentally. The proposed approach makes use of the longitudinal stress wave responses collected at the end of strands induced by a mechanical impact at the other end. The six 8m-long post-tensioned concrete beams have been specially designed and constructed. For each beam, the different tension levels are applied. The impact tests are conducted. The results show that longitudinal frequency, elastic wave velocity, and elastic modulus are nonlinearly increased as the tensile force level increases. It is thus expected that the longitudinal vibration characteristics of the existing bonded tendons can be of promising indicators for the inspection of a tensile force loss.

INTRODUCTION

Primary objective of nuclear containments is to prevent a leakage of a radioactive substance in the event of an extreme loading. In order to prevent such leakage and maintain a high level of integrity for such important structures, a prestressed concrete (referred to as PSC hereafter) has been widely used. However, time dependent loss of a prestressd force on tendons embedded in PSC is inevitable due to both creep and shrinkage of concrete and relaxation of tendons. Thus, most of regulations and guidelines of nuclear related structures have specified a periodic in-service inspection of tendon force.

For unbonded tendons in the containments, average tendon force can be evaluated by measuring the elongation at the end of active tendon induced by an applied jacking force [1]. For bonded tendons, however, direct estimation of tendon force is not feasible because of cement grouting between tendon and duct. Accordingly, alternative approaches have been proposed for the periodic in-service inspection of the containments with bonded tendons. US RG 1.9 [2] has suggested a lift-off measurement for unbonded sample tendons and a deformation measurement for the containments during periodic full scale pressure tests. Pandey [3] has proposed a reliability-based assessment of integrity of bonded prestressed concrete containments. The study has recommended that inspection results of lift-off, flexural and destructive tests for a set of beam specimens can be used in order to update the probability distribution of the prestressing force and the number of degraded tendons on the containments. Sun et al. [4] have also studied strength monitoring of a prestressed concrete containment with grouted tendons. Work done by Sun et al. [4] has utilized a real time monitoring system for overall containment deformation of such structure. However, the above approaches are neither fully satisfactory for strength monitoring of tendons nor promising methods for ensuring the structural integrity of containments and tendons.

A measurement of the tendon force has been achieved in terms of using a low and a high frequency approach. Whereas the former is in the range of vibration frequency level, the latter is in the range of ultrasonic frequency level. For a bridge cable, the existing tensile force on the bridge cable or a hanger can be evaluated by applying

T. Proulx (ed.), *Dynamics of Civil Structures, Volume 4*, Conference Proceedings of the Society for Experimental Mechanics Series 13,
DOI 10.1007/978-1-4419-9831-6_3, © The Society for Experimental Mechanics, Inc. 2011

the frequency-based system identification algorithm to the measured flexural frequencies [5]. For the unbounded PSC beam, tensile force and flexural rigidity can be evaluated by measuring the displacement, strain, and load time histories of the beam [6]. This is based on the results of Saiidi et al. [7] reporting that flexural natural frequencies increase as the applied compressive force on tendon increases. Without experimental verifications, however, Hamed and Frostig [8] have insisted that the flexural natural frequencies of a PSC beam are irrelevant not only to the applied tension force but also to the grouting conditions. Thus, the above two research results conflict each other.

Meanwhile, the high frequency approach is based on the physical phenomenon that the velocity of stress wave on a rod or a strand relies on the applied stress level. Chen and Wissawapaisal [9] have estimated the tensile stress on seven-wire strand by means of detecting the arrival group velocity of stress wave at one end of the strand after injecting longitudinal ultrasonic stress wave (150kHz~350kHz) at the other end of the strand. In addition, using magnetostrictive ultrasonic transducers, Kwun et al. [10] have also reported the existence of notch frequency (75 kHz~110 kHz) that is a disappeared frequency induced by the applied stress level in a seven-wire strand. Using the same concept of the arrival velocity difference on a stress field, Scalea et al. [11] and Chaki and Bourse [12] have conducted a similar pulse-echo technique utilizing magnetostrictive guided ultrasonic waves.

However, it is not feasible to apply such high frequency methods to the case of bonded tendon. This is due to the fact that the cement grouting surrounding steel tendons causes significant energy attenuation. Moreover, for the bonded tendons, it is known that the maximum inspection range of ultrasonic waves is less than 1.5m [13] while the typical height of nuclear containments is over 40m. Subsequently, no attempt has been made to directly evaluate tensile forces on the bonded tendons.

Since the first nuclear power plant was constructed in 1978, 20 unit nuclear power plants have currently been operated and maintained in Korea [14]. Among such nuclear containments, only Wolsong Units 1,2,3,4 and Ulchin Units 1, 2 were designed as prestressed concretes with bonded tendon systems. Since Wolsong Units started a commercial service in 1983, 30 years of design life time has now been approaching. Consequently, Korea Hydro Nuclear Power Company (KHNP) that owns the plant now concerns an important pending problem for continuous operation beyond the design life. Accordingly, the periodic in-service inspection has been arranged for Wolsong Units and a long-term research project has been designed to assess directly the effective prestress force on the bonded tendons embedded in the nuclear containments using nondestructive techniques. For this purpose, the indirect test beam method by Pandey [3] has been employed and thus a number of test beams have been prepared. The present study therefore represents the first feasible study of the research project.

Main objective of this study is to investigate a feasibility for nondestructively evaluating prestress force on bonded tendons embedded in the nuclear containments. Since the previous high frequency pulse approach has a strict limitation on energy attenuation in the case of bonded tendons, the current study focuses primarily on the utilization of low frequency pulse method. Rationale behind using the low frequency pulse method is due to the fact the low frequency propagates a long distance regardless of grouting conditions.

LONGITUDINAL VIBRATION TEST

Figure 1 shows the typical test set-up for the longitudinal vibration test. To excite the longitudinal modes of the specimens, an impact hammer, PCB Piezotronics model of 086C04, has been used. Acceleration responses caused by the impact hammer have been collected by PCB Piezotronics model of 352B10. Use is made of NI model CRIO-9073, four channels of NI 9233 and a laptop computer for data acquisition. In order to avoid an electric noise, two parallel 12 Volt batteries are employed as a power supply of the acquisition facilities. A sampling ratio of 50 kHz is utilized for the collections of the data.

A total six PSC beam specimens with bonded strands have been tested in the present study. Layout of the specimens is shown in Fig. 1, and dimension details and material properties of six specimens are summarized in Table 1. The PSC beams represent mock-up specimens of vertical walls for nuclear containments with unit width.

A B-type of KSD 7002 seven-wire strand is installed at the center of a concrete cross section. Nominal diameter, area and ultimate strength of the strand are 15.2mm, 138.7mm^2 and 260.68 kN, respectively. A VSL three hole-wedges system of P 6-3 anchors is installed. Internal and external diameters of the duct are 51mm and 54mm,

respectively. After applying tensile force on the strands, the space between duct and strands is filled with cement paste grouting. Three cylinder tests of grouting materials are carried out and average compressive strength is 71.7MPa. In addition, characteristic tests of concrete materials being used for specimens are conducted, and average values of elastic modulus and Poisson's ratio are 32,644MPa and 0.22, respectively.

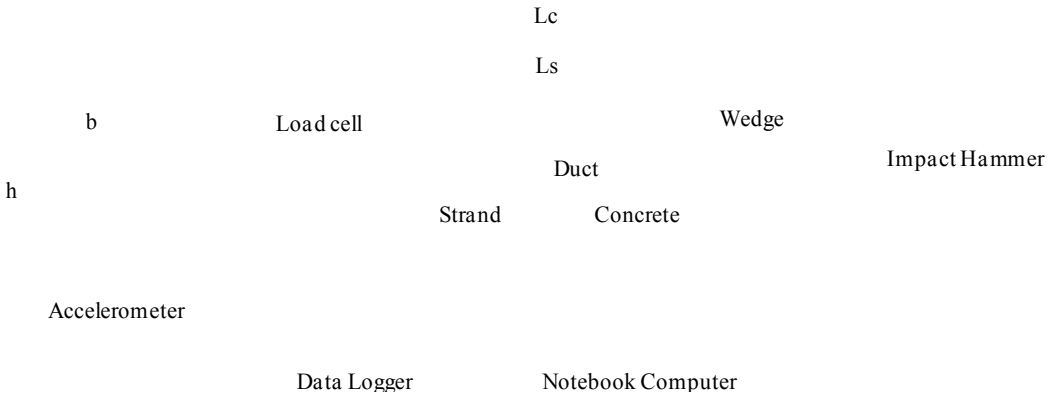

Fig.1 Test Specimen

Table 1. Test Specimens

PSC No.	Concrete				Strand			Remark
	Length Lc(m)	Width b(m)	Height h(m)	Strength (MPa)	Length Ls(m)	Anchor (VSL Type)	Tension T(kN)	
1	7.999	0.302	0.302	37.08	8.278	P 6-3	0.0	0
2	8.000	0.303	0.301	37.08	8.439	P 6-3	145.6	19% Tu
3	7.995	0.300	0.300	37.08	8.444	P 6-3	263.8	34% Tu
4	7.994	0.302	0.301	37.08	8.433	P 6-3	355.8	46% Tu
5	7.998	0.303	0.299	37.08	8.435	P 6-3	465.0	59% Tu
6	7.993	0.303	0.302	37.08	8.433	P 6-3	522.5	67% Tu

All of specimens are assumed to be simply-supported by two roller conditions and a tensile force is introduced at one end of each specimen. A load cell has been installed in each of specimens in order to estimate the applied tensile force introduced on strands. Whereas a load cell of ZIS model, ELC-100S is employed for specimens.

Six tests have been carried out for the specimens. In the tests, three accelerometers are clamped at core wires since the specimens have three strands. An impact is loaded at the opposite side of accelerometers and arbitrary support locations are employed as illustrated in Fig. 2.

(a) (b)

Fig.2 Support Condition and Accelerometer Locations in Test No.4: (a) supports; (b) accelerometers

EXPERIMENTAL RESULTS

Longitudinal impact tests of 160 times are repeatedly conducted for each specimen. A typical impact time history is collected with the sampling rate of 50 kHz as shown in Fig.3a. Averaged power spectrum of acceleration responses is evaluated using Hanning window and is depicted in Fig. 3b. To obtain the spectrum, 2^{13}, 2^{14} and 1.562Hz are employed for a data length, a number of FFT and a frequency solution, respectively. As observed from the spectrum, the impact has been excited up to 6 kHz.

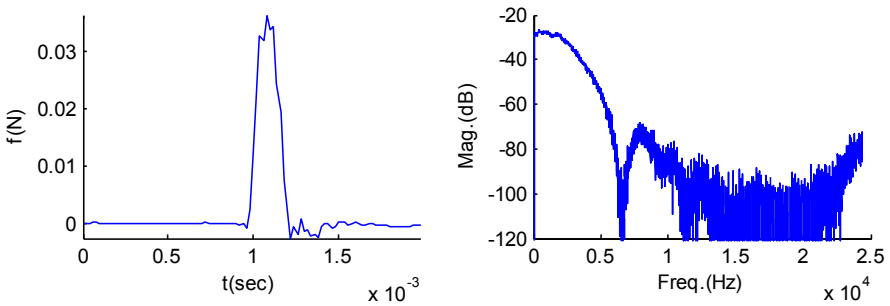

(a) (b)

Fig.3 Typical Impact Signal: (a) time history; (b) frequency spectrum

For each specimen and the resulting transfer functions are illustrated in Fig. 4. It is observed in general that magnitudes of transfer functions in the frequency band of 4 to 5 kHz increase as the applied tensile force level increases. In addition, a number of noticeable peaks in the transfer function of PSC specimen No. 6 is more than 30, while those in the transfer function of PSC specimen No. 1 is at most 8. This can be attributed to the introduced tensile force level on the specimens. As the tensile force is increased, axial force level is also increased. This leads to an increase in both stiffness and strength of the specimens, but a decrease in internal damping.

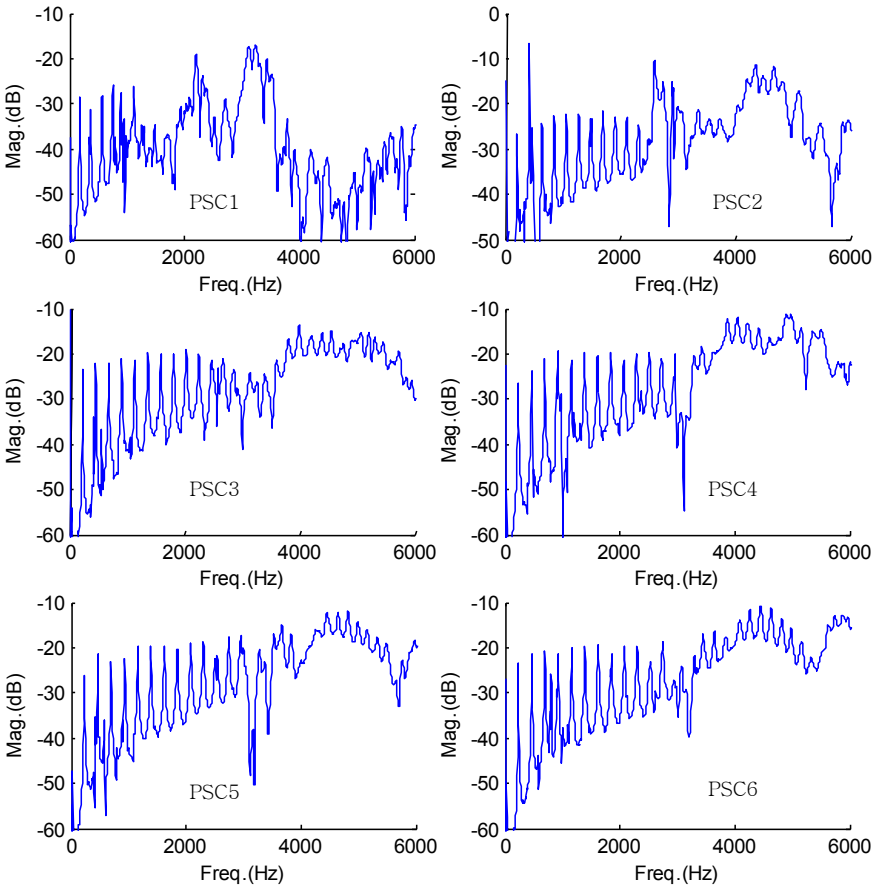

Fig. 4 Longitudinal Natural Frequency and Applied Tension

In order to investigate the longitudinal natural frequency, a simple equation is employed for the calculation of theoretical longitudinal frequency. For a homogeneous axial member with free-free boundary conditions, the *n*th theoretical longitudinal natural frequency in Hz is obtained by.

$$f_n = \frac{n\, c_0}{2L} \tag{1}$$

$$c_0 = \sqrt{\frac{E}{\rho}} \tag{2}$$

where L, c_o, E, and ρ denote length of a member, elastic wave velocity, elastic modulus, and mass density for the condition of no tension, respectively. To compute theoretical longitudinal frequencies, the wave velocity of PSC specimen No. 1 is firstly identified using the known length given in Table 1 and the first measured natural frequency. This is reasonable since no tension is applied to the PSC specimen No. 1. Calculated wave velocity is 2930.4 m/s. Then, the *n*th higher modes are generated in terms of multiplying the wave velocity by *n*. For the case of no tension, the measured eight frequencies agree very well with the predictions. This implies that the existing linear theory in Eq. (1) is based on a constant wave velocity assumption. Extracted longitudinal natural frequencies of the specimens are shown in Fig. 5. It is clearly observed that the longitudinal natural frequencies are increased when the applied tensile force level increases. This leads to the fact that the longitudinal natural frequency depends on the introduced tensile force level.

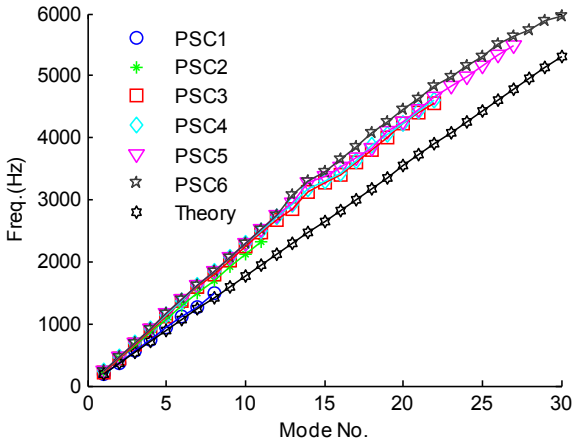

Fig.5 Extracted Natural Frequency

DISCUSSIONS

Frequency and Tension

For all PSC specimens, longitudinal natural frequencies extracted by a peak-peaking technique are summarized in Table 2. It is obvious from the Table 2 that the frequencies are increased as the applied tensile force level increases. This has been graphically represented in Fig. 6 which shows variations of frequencies with reference to the applied tensile force levels for various modes. In general, the frequencies vary linearly with tensile force in relatively low levels of the applied tension.

Table 2. Extracted Natural Frequency

PSC No.	Frequency (Hz)							
	1	2	3	4	5	6	7	8
1	177.0	366.2	567.6	750.7	939.9	1117	1257	1483
2	207.5	427.2	640.9	854.5	1068	1282	1483	1703
3	225.8	451.7	677.5	903.3	1129	1361	1587	1807
4	231.9	463.9	689.7	921.6	1154	1379	1611	1837
5	231.9	463.9	689.7	927.7	1160	1385	1624	1843
6	231.9	463.9	695.8	927.7	1160	1392	1624	1855

However, the frequencies increase asymptotically in high levels of the applied tension. This suggests that the frequencies can be a sensitive feature for PSC specimens with a level of the applied tension. In addition, for higher modes (i.e., from the 3rd mode), frequencies in high levels of the applied tension (approximately 50% of the ultimate strength of a strand) tend to be slightly increased as the mode is increased. This phenomenon is particularly important since typical tension levels of nuclear containments in practice are within a range of 60% to 70% of the ultimate strength of a strand. It is thus expected that a continuous monitoring of the longitudinal frequencies may enable change of tension levels to be identified.

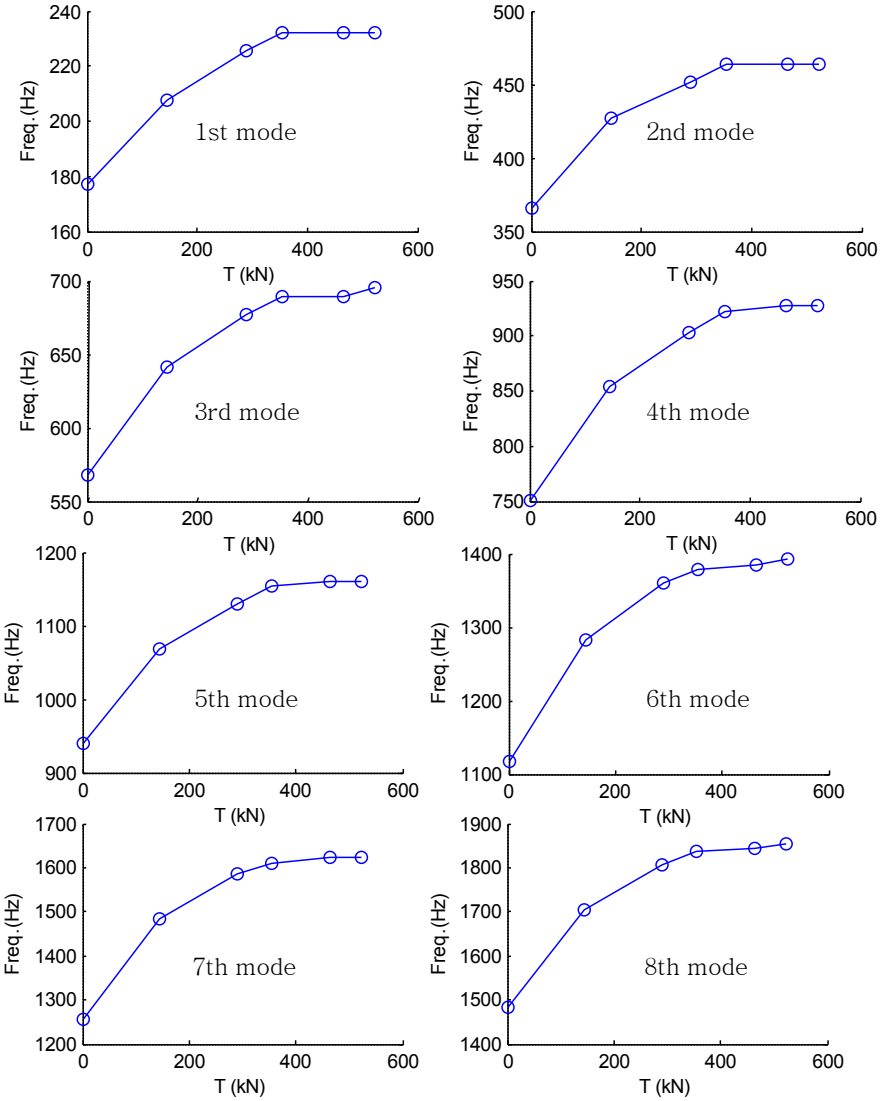

Fig.6 Longitudinal Natural Frequency and Applied Tension

Wave Velocity and Tension

An elastic wave velocity can be calculated for each mode in terms of substituting the measured frequency given in Table 2 and a specimen length into Eq. (1). Shown in Fig. 7 is a comparison of change rates for the estimated elastic wave velocities with respect to the case of no tension, i.e., PSC specimen No. 1. In general, change rates of elastic wave velocities are increased as the applied tensile force level increases. In particular, when the applied tensile force level is corresponding to 67% of the ultimate strength of a strand, the maximum increment rate of 33.5% occurs in the 1st mode and the minimum increment rate of 24.9% takes place in the 3rd mode. Meanwhile, in case that the applied tensile force level is reduced from 67% to 46% of the ultimate strength of a strand, little variation of elastic wave velocity is happened in the 1st mode, and a minor decrease of 1.24% in elastic wave velocity occurs in the 8th mode. This suggests that when the applied tension level is decreased approximately 30%, a variation in the elastic wave velocity is within a margin of a measurement error. Thus, the elastic wave velocity does not seem to be a feasible parameter for the identification of tension level variation.

However, in case that the applied tension level is further reduced from 67% to 19% of the ultimate strength of a strand, estimated elastic wave velocities in the 1st and 8th modes are reduced to 13.96% and 10.38% in comparison with those of no tension specimen, respectively. This indicates that, when an approximately 72% of reduction in applied tension level occurs, a variation rate of estimated elastic wave velocities seems to make the

tension levels to be identified. In short, tension levels can be identified in terms of using the variation rate of the elastic wave velocities, only for the case that the applied tensile force level is reduced in 30% or more.

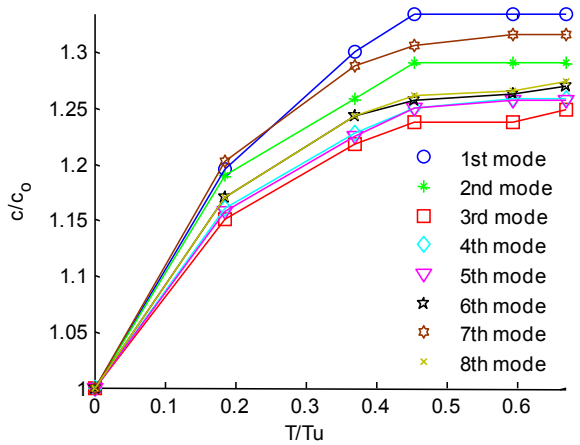

Fig.7 Change Rate of Elastic Wave Velocity and Applied Tension

Elastic Modulus and Tension

In the linear elastic theory of Eq. (1), a basic assumption is that the longitudinal natural frequency and elastic wave velocity do not vary with a change in the applied tension. However, experimental results demonstrate obviously that the natural frequency is nonlinearly increased as the applied tension level increases. Substituting Eq. (2) into Eq. (1), an elastic modulus can be given as follows.

$$E = \rho\left(\frac{2Lf_n}{n}\right)^2 \tag{3}$$

With the assumption that a small variation in the mass density is negligible, the elastic modulus relies on the mode number and longitudinal frequency. Since the frequency has a nonlinear relationship with the applied tension as illustrated in Fig. 6, the elastic modulus can also be relied on both the applied tension level and the mode number. This is supported by the research results of Kim and Park [5]. Work done by Kim and Park [5] confirmed that a flexural rigidity of a bridge cable is proportional to the applied tension on the cable.

Substituting the measured frequency listed in Table 2 and the mode number into Eq. (3), the elastic modulus of a strand can be achieved and summarized as Table 3. Use is made of an electronic scale for the mass density (7729.779 kg/m^3) of the strand. Coefficient of variation (COV) reveals that the variation of the estimated elastic modulus with respect to the modes is negligible, while it is sensitive to the applied tension level. Hence, the elastic modulus can be of more useful indicator for the change of the applied tension levels rather than frequencies and elastic wave velocities. This can be further supported by fact that the elastic modulus has a square sensitivity to the measured frequency as given in Eq. (3), while the elastic wave velocity has a linear sensitivity to the frequency in Eq. (1).

Table 3. Estimated Elastic Modulus (GPa) of Strand

PSC No.	Mode No.								Mean	COV
	1	2	3	4	5	6	7	8		
1	66.38	71.03	75.84	74.63	74.87	73.43	68.32	72.81	72.16	0.0464
2	94.81	100.5	100.5	100.5	100.5	100.5	98.83	99.78	99.48	0.0199
3	112.4	112.5	112.4	112.4	112.4	113.4	113.3	112.5	112.7	0.0039
4	118.2	118.3	116.2	116.7	117.1	116.1	116.5	115.9	116.9	0.0079
5	118.3	118.4	116.3	118.3	118.4	117.2	118.4	116.8	117.8	0.0074
6	118.2	118.3	118.3	118.3	118.3	118.3	118.3	118.2	118.3	0.0004

Assuming that the mass of density of concrete is 2450 kg/m^3, the elastic modulus of concrete has been evaluated and given in Table 4. A similar trend as the above case of a strand is achieved. In general, an estimated elastic modulus of a concrete specimen is insensitive to the mode number, while it is affected by the applied tension

levels. Graphical representation is given in Fig. 8 which demonstrates that normalized elastic moduli of both strand and concrete vary with the applied tension levels. In Fig. 8, E_o denotes the estimated elastic modulus of the PSC specimen No. 1 which has no tension. As observed, when the applied tension level of 67% is reduced to 59%, 46%, 34%, and 19% of the ultimate strength of a strand, average elastic modulus of the strand is decreased as much as 0.5%, 1.2%, 4.8%, 15.9%, and 39%, respectively, while that of concrete is diminished as much as 0.4%, 1.2%, 5.0%, 15.9%, and 37%, respectively. Taking into account approximately 5% of a measurement error, a change of the applied tension level can be of measurable when the applied tension level of 67% is reduced to 46% or less of the ultimate strength of a strand.

Table 4. Estimated Elastic Modulus (GPa) of Concrete

PSC No.	Mode No.								Mean	COV
	1	2	3	4	5	6	7	8		
1	19.6	21.0	22.4	22.1	22.2	21.7	20.2	21.5	21.4	0.0464
2	27.0	28.6	28.6	28.6	28.6	28.6	28.2	28.4	28.3	0.0199
3	31.9	32.0	31.9	32.0	31.9	32.2	32.2	32.0	32.0	0.0039
4	33.7	33.7	33.1	33.2	33.4	33.1	33.2	33.0	33.3	0.0079
5	33.7	33.7	33.1	33.7	33.7	33.4	33.7	33.3	33.6	0.0074
6	33.7	33.7	33.7	33.7	33.7	33.7	33.7	33.7	33.7	0.0004

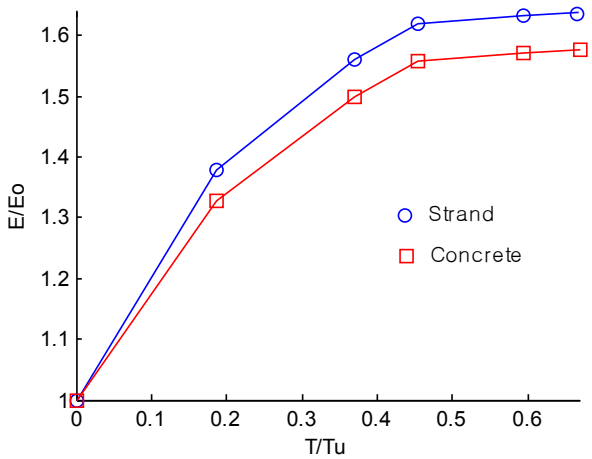

Fig.8 Change Rate of Elastic Modulus and Applied Tension

SUMMARY AND CONCLUSIONS

A feasibility study has been conducted for the evaluation of tensile force levels applied on grouted tendons which are embedded in nuclear containments. For this purpose, an experimental programme has been carried out for PSC specimens subjected to longitudinal vibration of an impact. Based on detailed analyses and evaluation for experimental responses of acceleration time histories and power spectrums, the following conclusions can be made.

In the existing linear theory, longitudinal natural frequency, elastic wave velocity, and elastic modulus are independent of the applied tension. However, this may not be true since present experimental results demonstrate that there is a functional relationship between them. The results show that they are nonlinearly increased as the applied tensile force level increases. In addition, present study proves that variation rates of the applied tension levels are noticeable in elastic modulus rather than in either frequency or elastic wave velocity. Hence, the elastic modulus can be of the most promising parameter for the identification of the applied tensile force level. It is thus expected that monitoring the longitudinal vibration responses enables the applied tension level on the grouted tendon embedded in a nuclear containment to be accurately captured.

However, there is certainly a room for improvements of the present study if experimental study is extensively carried out for further analyses of longitudinal vibration responses.

ACKNOWLEDGEMENTS

This research is sponsored by the Korean Ministry of Science and Technology under the National Mid-term and long-term Atomic Energy R&D Program.

REFERENCES

[1] Anderson, P., Berglund, L.E., 2005. Average force along unbounded tendons: a field study at nuclear reactor containments in Sweden. Nuclear Engineering and Design, Vol.235, pp. 91-100.
[2] USNRC, 1990, Determining Prestressing Forces for Inspection of Prestressed Concrete Containments. RG 1.35.1.
[3] Pandey, M.D., 1997. Reliability-based assessment of integrity of bonded prestressed concrete containment structures, Nuclear Engineering and Design, Vol.176, pp. 247-260.
[4] Sun, Z., Liu, S., Lin, S., Xie, Y., 2002. Strength monitoring of a prestressed concrete containment with grouted tendons. Nuclear Engineering and Design, Vol. 216, pp.213-220.
[5] Kim, B.H. and Park, T. (2007) Estimation of cable tension force using the frequency-based system identification method. *Journal of Sound and Vibration*, Vol. 204, pp. 660-676.
[6] Law, S.S. and Lu, Z.R. (2005) Time domain responses of a prestressed beam and prestress identification. *Journal of Sound and Vibration*, Vol.288, pp. 1011-1025.
[7] Saiidi, M., Douglas, B. and Feng, S. (1994) Prestress force effect on vibration frequency of concrete bridges", *Journal of Structural Engineering*, ASCE, Vol. 120, No. 7, pp. 2233-2241.
[8] Hamed, E. and Frostig, Y. (2006) Natural frequencies of bonded and unbonded prestressed beams-prestress force effects. *Journal of Sound and Vibration*, Vol. 295, pp. 28~39
[9] Chen, H.L., Wissawapaisal, K. (2002) Application of Wigner-Ville Transform to evaluate tensile forces in seven-wire prestressing strands. *Journal of Engineering Mechanics*, ASCE, Vol. 128, No. 11, pp. 1206-1214.
[10] Kwun, H. Bartels, K.A. and Hanley, J.J. (1998) Effects of tensile loading on the properties of elastic-wave propagation in a strand. *Journal of Acoustic Society of America*, Vol.103, No.6, pp. 3370-3375.
[11] Scalea F L, Rizzo P, and Seible F, “Stress measurement and defect detection in steel strands by guided stress waves”, Journal of Materials in Civil Engineering, ASCE, 2003 15(3) 219-227.
[12] Chaki S and Bourse G, “Guided ultrasonic waves for non-destructive monitoring of the stress levels in prestressed steel strands”, Utrasonics, 2009 49(2) 162-171.
[13] Beard M D, Lowe M J S, and Cawley P, “Ultrasonic guided waves for inspection of grouted tendons and bolts”, Journal of materials in civil engineering, ASCE, 2003 15(3) 212-218.
[14] Park, J. Hong, J., 2009. Present status of nuclear containments and ISI in Korea, Progress in Nuclear Energy, doi:10.1016/j.pnucene.2009.05.005, article in press.